

Article

Clusters of Shaped Ultrasonic Transducers for Lamb Waves' DoA Estimation

Marco Dibiase ¹  and Luca De Marchi ^{2,*}

¹ Department of Computer Science and Engineering, University of Bologna, 40136 Bologna, Italy; marco.dibiase3@unibo.it

² Department of Electrical, Electronic, and Information Engineering "Guglielmo Marconi", University of Bologna, 40136 Bologna, Italy

* Correspondence: l.demarchi@unibo.it; Tel.: +39-051-2093777

Received: 27 October 2020 ; Accepted: 14 November 2020; Published: 17 November 2020



Abstract: The direction of arrival (DoA) estimation of Lamb waves is a fundamental task to locate acoustic events, such as those caused by impacts in plates or shells. To perform this task, a novel cluster of piezoelectric sensors is presented in this work. The designed cluster is composed by three irregularly shaped patch transducers (P1, P2 e P3). This is in contrast with the approaches that are typically presented in literature which are based on isotropic piezo-disks. In our approach, the transducers are shaped with a procedure based on the Radon Transform, so that the difference in time of arrival (DToA) of the Lamb waves at patches P1 and P2 is linearly related to the DoA, while P3 is designed so that it is possible to perform the estimation of DoA without knowing the actual wave velocity. The numerical validation shows that the performance in the DoA estimation achieved by means of the proposed cluster compares favorably with respect to clusters of conventional sensors, even in the case of noise-affected measurements.

Keywords: direction of arrival estimation; Acoustic source location; piezoelectric sensors; shaped sensors; Lamb waves; Radon transform

1. Introduction

Structural Health Monitoring (SHM) systems [1], i.e., inspections systems based on permanently installed sensors, have been intensively investigated in recent years, due to the high potential that they have in reducing maintenance costs in a wide range of industrial application fields. In particular, an increasing demand to develop SHM systems comes from the automotive and aerospace industries [2]. In these fields, open challenges are: (i) the reduction of the monitoring system weight (including the associated cabling and circuitry), the minimization of both (ii) the power consumption, and (iii) the amount of data that are to be transferred and processed

Among the various sensor technologies proposed for SHM, those that are based on the usage of ultrasonic guided waves (GWs), are considered to be particularly attractive because of the GW property to travel across long distances with low attenuation. In particular, passive GW methods can be used to detect and locate acoustic sources (AS) in plates or shells, such as those that are generated by impacts, or acoustic emissions generated by cracks and corrosion, by using piezoelectric sensors [3,4].

The approaches presented in literature for AS localization with GW can be divided in three main groups: (i) inverse methods [5,6], (ii) hyperbolic location methods [7], and (iii) methods that use Direction of Arrival (DoA) estimations [8,9]. However, if the first two methods are well validated at laboratory scale, these approaches are rarely adopted for field deployment, because of the stringent hypotheses that they rely on. In particular, the first group implies onerous calculations because it requires a very accurate modeling of the guided ultrasonic propagation, whereas the second group

requires a large number of sensors in order to reduce the estimation uncertainty. Moreover, this latter approach is unsuitable when the wave propagation characteristics vary in the monitored area. For these reasons, the methods belonging to the third group, which estimate DoAs by using clusters of closely located sensors that do not rely on the knowledge of the characteristics of propagation, are often the only viable strategy to locate AS with embedded systems.

Kundu et al. in [9,10] proposed a simple cluster of 3 circular sensors. In this work, this solution will be referred to as “conventional cluster”. The DoA is performed by estimating the Difference in Time of Arrival (DToA) of wave-fronts between sensors. The DToAs, i.e., the time delays, can be estimated with conventional cross-correlation procedures (i.e., the optimal method for measurements that are affected by additive white Gaussian noise N_{W_G} with zero mean [11]). This cluster typology allows for estimating the DoA with minimum amount of data to acquire (only three signals) and reduced computational cost (only two time delays estimations). Such an approach was proven to be suitable for real-field applications to perform real-time impact detection and localization [10]. It is worth noting that Park, Packo, Kundu, and Sen in [12,13] showed that it is possible to estimate the AS localization even in the case of heavily anisotropic structures (i.e., characterized by elliptical or rhomboidal wave fronts).

In this work, we further investigate the concept of DoA detection via DToAs estimations, by analyzing how beneficial the adoption of clusters constituted by irregularly shaped piezoelectric transducers can be. In particular, in the proposed approach, the sensors are shaped with a procedure based on the Radon Transform (RT) and its Inverse (IRT). This procedure allows to define the DToA between two sensors as an arbitrary DoA function, divided by the wave velocity v , as better detailed in Section 3. The RT approach was firstly presented in [14] in order to estimate the DoA by using two shaped sensors when the actual wave velocity is assumed to be known. In another previous work [15], the concept has been extended to the case of unknown velocity of propagation, designing a cluster with three shaped sensors. It is worth noting that the relationship between DToA and DoA affects the uncertainty in DoA estimation. In this paper, we define a new cluster of three shaped sensors in order to further reduce the uncertainty with respect to [15]. The conducted numerical tests show that the DoA estimation performed by the new cluster is more accurate than the one achieved with the conventional cluster or with the cluster proposed in [15], and it is robust, even when the measurements are affected by noise or acquired at low sampling frequencies. It is also worth noting that the computational cost that is associated to the processing of the shaped cluster signals for DToA estimation is fully equivalent to the one of conventional clusters, while the DoA estimation is even simpler because it purely linear w.r.t the DToAs ratio, while the conventional approach is based on trigonometric functions.

The experimental validation of the shaping concept is beyond the scope of this paper. Nevertheless, it is worth mentioning that the proposed cluster of shaped sensors can be realized by relying on different piezoelectric materials and manufacturing techniques. e.g., metallized PVDF (polyvinylidene fluoride) sheets can be used by shaping the electrodes on the upper surface with a laser cut as in [16]. Alternatively, the shaping strategy can be based on printing metallic electrodes on PVDF films in order to obtain the desired shape sensors, as proposed in [17], or by using lithographic procedures as in [18]. In the practical adoption of these devices, a fundamental step is the definition of a well controlled bonding procedure, because it may heavily affect the sensor response [19].

The paper is organized, as follows. In Section 2, by exploiting the Propagation of Uncertainty theory [20], the functions that bind the DoA to the Differences in Time of Arrival (DToAs) of the wavefront at piezo-patches P1 and P2, and at P1 and P3, are defined to reduce the uncertainty in DoA estimation, when the wave mode velocity is not known. Section 3 shows how to implement the desired functions by properly shaping the sensors in the context of guided waves, in particular of Lamb waves. To this aim, the Radon Transform and its inverse are introduced. Section 4 validates the theoretically expected performances with numerical simulations. The estimation of the DoA is simulated in challenging working conditions, i.e., with noisy measurements or very low sampling

frequencies, to emulate real field acquisitions. Moreover, a numerical comparison between the shaped sensors cluster and the conventional cluster is provided. Finally, Section 5 depicts the conclusions.

2. Minimization of Uncertainty in Doa Estimation

The simplest sensor configuration to perform the wave DoA estimation is based on a couple of isotropic transducers, i.e., the piezopatches P1 and P2 illustrated in Figure 1. Assuming a planar wavefront, the Difference in Time of Arrival (DToA, Δt) is related to the wave DoA (θ) by this formula:

$$\Delta t(\theta) = \frac{d \cdot \cos \theta}{v} \tag{1}$$

where d is the distance among the sensors and v is wave velocity. Consequently, the estimation of the DoA can be performed from the measured DToA (Δt_{est}) by applying the inverse formula:

$$\theta_{est} = \arccos \frac{v \cdot \Delta t_{est}}{d} \tag{2}$$

The Propagation of Uncertainty theory [20] that is applied to this case reveals that the error in the estimation can be very large for low values of θ . This is due to the non-linear characteristics of the \arccos relation. To counteract this problem, in [14], a sensor reshaping procedure was proposed in order to achieve a linear dependence between the DToA and the DoA, so that:

$$\Delta t_{12}(\theta) = \frac{\alpha \cdot \theta + \rho_0}{v} = \frac{\rho_2(\theta)}{v} \tag{3}$$

where ρ_0 and α can be chosen by the designer. Thanks to new linear relation, the worst-case error is constant over the considered range of angles ($\theta \in [0^0, 90^0]$), and it is considerably lower than the maximum error that is achieved using the conventional sensors. It is worth noting that the worst case error is inversely proportional to the selected value of α . For this reason, the larger α the lower is the error in the DoA estimation; however, there is a trade off involved in the selection of α , because, the larger is α , the larger are the physical dimensions of the piezoelectric patches and the maximum value of the DToA, which defines the time-window length of the acquired signal (i.e., the information to be stored and processed).

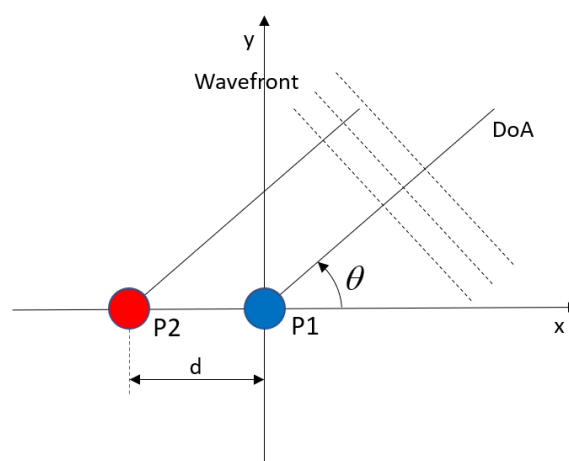


Figure 1. A basic cluster of two circular piezo-sensors spaced apart by a distance d .

It is also worth noting that a cluster that is composed by two sensors can be used to estimate θ just if the actual wave velocity v is assumed to be known. Therefore, if the velocity is not known a

priori, a third sensor P3 is needed in order to estimate the DoA. In the proposed approach, the sensor P3 is shaped, so that it establishes a constant reference to estimate the wave velocity, i.e.,

$$\Delta t_{13}(\theta) = \frac{\rho_3(\theta)}{v} = \frac{\rho_{3c}}{v} \tag{4}$$

(where ρ_{3c} is a constant), the relation between the DToAs ratio and DoA is:

$$\frac{\Delta t_{12}}{\Delta t_{13}} = \frac{(\rho_0 + \alpha\theta)}{\rho_{3c}} = \frac{\rho_2(\theta)}{\rho_{3c}} \tag{5}$$

In the last equation, it can be observed that the DoA θ is linked to the ratio of DToA by a simple linear relation. Moreover, in order to estimate the DoA, the knowledge of the wave propagation velocity is not necessary, because such quantity does not appear in (5). However, the third sensor P3 introduces an additional uncertainty in the DoA estimation due to Δt_{13-est} .

In particular, the worst case error can be very large when the DoA is around 90 [deg], if ρ_0 is set to 0. The Figure 2a shows the upper and lower bounds of worst case error for the shaped sensors cluster proposed in [15]. It was designed for a work-range of [0, 90] [deg] and it was defined by the following parameter values: $d = 20$ [mm], $\alpha = d/90$ [deg] $\simeq 0.22$ [mm/deg], $\rho_0 = 0$ [mm], $\rho_{3c} = -7$ [mm]. The value of d defines the maximum absolute value of DToA, equal to d/v (in this case, obtained when $\theta = 90$ [deg], for piezo P2). Therefore, the value of d is redefined as the Maximum Difference in Distance of Propagation (MDDP). It is worth noting that the MDDP, d , in general, does not correspond to the physical distance between the shaped sensors. The error bounds were computed and illustrated for all of the clusters here considered by setting the value of the wave velocity $v = 2000$ [m/s] and DToAs Standard Deviation equal to 2 [μ s].

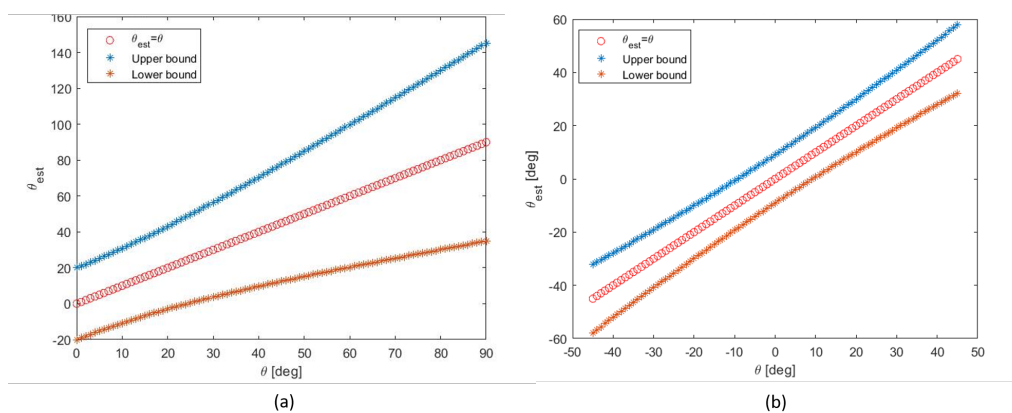


Figure 2. Upper and lower error bounds of two clusters of three shaped sensors to estimate the direction of arrival (DoA), when the wave mode velocity is unknown: (a) the case of the cluster presented in [15]. (b) The new cluster of three shaped sensors.

The worst case error can be reduced by selecting an appropriate value for ρ_0 (i.e., ρ_0 so that $\rho_2(45^\circ) = 0$), or by working on a shifted range of angles, centered on the zero angle, i.e., $\theta \in [-45^\circ, 45^\circ]$. In this case, the parameters α, ρ_0 and ρ_3 can be used in order to minimize the uncertainty in DoA estimation. In particular, ρ_0 should be equal to 0, while α and ρ_{3c} are defined by selecting the maximum absolute values of $\Delta t_{12}(\theta), \Delta t_{13}(\theta)$, i.e., d/v , equal to the maximum absolute values of DToAs for the conventional cluster. Limiting $\Delta t_{12}, \Delta t_{13}$ implies the limitation of the maximal dimensions of the transducers, and also the relaxation of memory requirements for the storage and subsequent

cross-correlation of the acquired time-waveforms. To summarize, the values of the parameters $\alpha, \rho_0, \rho_{3c}$ and the functions $\rho_2(\theta), \rho_3(\theta)$ are:

$$\begin{aligned} \alpha &= d/45[\text{deg}], \quad \rho_0 = 0, \quad \rho_{3c} = d \\ \rho_2(\theta) &= \alpha \cdot \theta, \quad \rho_3(\theta) = \rho_{3c} \end{aligned} \tag{6}$$

In particular, the new shaped sensors cluster was designed, so that the MDDP is again $d = 20$ [mm]. Figure 2b illustrates the worst-case error for this configuration, in terms of upper and lower bounds.

Figure 3b shows the upper and lower bounds of the conventional cluster with three circular sensors [9,10] with the MDDP equal to $d = 20$ [mm] (this distance corresponds, for the circular sensors, to the physical distances between sensors in Figure 3a). The cluster of shaped sensors that implements the relations (3) and (4) with the parameters being detailed in Equation (6) allows for a theoretical average reduction of the worst case error of 11%. It is important to stress the fact that the comparison is provided with the same maximum absolute value for the DToAs (i.e., d/v). This means that the two clusters have the same memory requirements and same computational cost to estimate the time delays. It is also worth highlighting that the two clusters differ considerably in terms of DoA estimation function: the conventional cluster requires the evaluation of the *atan* function of the DToAs ratio, while the estimation function of the new cluster is simply linear w.r.t. the DToAs ratio. It is given by inverting (5) with respect to θ . Therefore it is compatible with embedded systems that are equipped with micro-controller units.

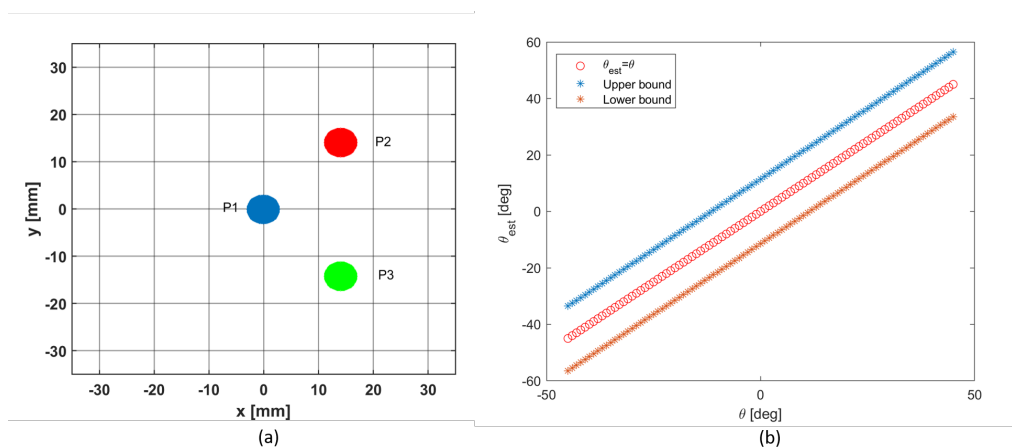


Figure 3. (a) The conventional cluster of 3 circular piezo-sensors spaced apart by a distance $d_{CC} = 20$ [mm]. (b) Upper and lower error bounds of the conventional cluster.

Unfortunately, implementing a cluster of piezo-patches that are characterized by the DToA-DoA relationships in (5) and (6) is not possible with simple piezo-disks. Shaped sensors have to be used, but this introduces an additional complication: in fact, shaped sensors are generally characterized by an angle-dependent wavenumber tuning effect [19], i.e., the frequency response of the transducer depends on the direction of propagation of the incident wave. In turn, this effect may hamper the possibility to extract the time difference of arrival with conventional cross-correlation procedures, in which the response among different transducers is assumed to be the same. In the next section, the method that was proposed in [14] to tackle this problem is reviewed and applied to the considered three-sensor cluster case.

3. The Radon Transform as Sensor Shape Design Tool

The goal of having transducers with the desired relations (3) and (4), is achieved if the sensors are shaped so that the angle-dependent frequency responses $V_{P2}(\omega, \theta)$ and $V_{P3}(\omega, \theta)$ (of P2 and P3, respectively) are linked to $V_{P1}(\omega)$ (i.e., the isotropic one of the reference circular sensor P1), so that:

$$\begin{aligned} V_{P2}(\omega, \theta) &= V_{P1}(\omega) \exp(-jk_0(\omega)\rho_2(\theta)) \\ V_{P3}(\omega, \theta) &= V_{P1}(\omega) \exp(-jk_0(\omega)\rho_3(\theta)) \end{aligned} \tag{7}$$

i.e., the frequency response of the three piezo patches should be equal but for a phase shift which is proportional to the ρ_2 and ρ_3 quantities which we have introduced in the previous section. The term $k_0(\omega)$ is the wave vector-frequency relationship of a guide wave mode, i.e., the so called dispersion curve of the Lamb wave that is captured by the sensor. Replacing $k_0(\omega)$ with $\omega/v(\omega)$ where $v(\omega)$ is the phase wave velocity, under the hypothesis of narrow-band waves, the variations of $v(\omega)$ can be neglected and, given ω_0 the center frequency, a constant velocity $v(\omega_0)$ can be considered. The relationships (7) then create the relationships (3) and (4) over time.

To impose the relationships (7) three key elements can be exploited:

- (a) The model of the frequency response of a sensor in the presence of a Lamb wave mode.
- (b) The Radon Transform (RT) and its inverse (IRT).
- (c) The Projection Slice Theorem.

For the element (a), the model that was proposed by Senesi and Ruzzene [21] can be adopted:

$$V_P(\omega) = jU(\omega)k_0(\omega)H_P(\theta)D_P(\omega, \theta) \tag{8}$$

where $U(\omega)$ denotes the amplitude and the polarization of the wave component relevant to the piezo properties of the patch at the considered frequency, $k_0(\omega)$ is the wave vector that characterizes the propagation, $H_P(\theta)$ is a quantity that is related to the material properties of the piezo-structure system, and finally $D_P(\omega, \theta)$ is the sensor Directivity function, which is the only function that is dependent on the shape of the sensor. It can be computed by the following integral:

$$D_P(\omega, \theta) = \int_{\Omega_P} e^{-jk_0(\omega)(x \cos \theta + y \sin \theta)} \phi_P(x, y) dx dy \tag{9}$$

where $\phi_P(x, y)$ is referred to as shape function and it describes the shape of sensor as a step function of form:

$$\phi_P(x, y) = \begin{cases} 1 & (x, y) \in \Omega_P \\ 0 & (x, y) \notin \Omega_P \end{cases} \tag{10}$$

with Ω_P the area of the piezoelectric path. Without lack of generality, here we consider the case of a single piezoelectric patch, with a single polarization and constant piezoelectric properties. From Equation (9), the Directivity function can be computed as the bidimensional Fourier Transform (FT) at the angle θ of the shape function $\phi_P(x, y)$. Furthermore, the output variable is evaluated in $k_0(\omega)$, the wave vector of the Lamb wave mode considered (e.g., A_0, S_0 , etc. modes).

The element (b), which is the Radon Transform [22], is defined, as follows:

$$R_\theta(\rho)[\varphi(x, y)] = \int \int_{\Omega_P} \phi(x, y) \delta(\rho - x \cos \theta - y \sin \theta) dx dy \tag{11}$$

and it consists of multiple line-integrals. It admits inverse.

Finally (Point (c)), the Projection Slice Theorem [23] states that the bidimensional FT at the angle θ of a given function, is equal to the mono-dimensional FT of the Radon Transform of that function. This implies that the Directivity function, and therefore the frequency response, can simply

be calculated as the monodimensional FT of the RT of the shape function and by evaluating into $k_0(\omega)$. As a consequence, the relations (3) and (4), i.e., (9) in frequency, with $\rho_2(\theta)$ and $\rho_3(\theta)$ specified in (6) are obtained by imposing two suitable relations between the RT of sensor P1 and the RT of sensors P2 and P3:

$$\begin{aligned} R_\theta(\rho)[\varphi_2] &= R_\theta(\rho - \rho_2(\theta))[\varphi_1] \\ R_\theta(\rho)[\varphi_3] &= R_\theta(\rho - \rho_3(\theta))[\varphi_1] \end{aligned} \tag{12}$$

In conclusion, the synthesis procedure of the shape functions for sensors P2 and P3, which realizes the cluster of the desired re-shaped sensors, can be summarized, as follows: consider an isotropic circular reference sensor 1, then calculate its RT (constant over θ) and impose the RT of sensors P2 and P3 by using (12) with $\rho_2(\theta)$ and $\rho_3(\theta)$ given by (6) (see Figure 4a,b). In particular, the shaped sensors cluster was designed with $d = 20[\text{mm}]$ (the Maximum Difference in Distance of Propagation).

By inverting these two RTs, we obtain two shape functions that are continuously modulated (Figure 4c,d). In order to obtain two step functions, as in (10), a quantization procedure is imposed by setting all values greater than a certain threshold to 1 and the others to 0. In this way, the desired shape (step) functions can be obtained (as illustrated in Figure 4e,f).

Figure 4g,h shows the actual RTs (i.e., the RTs computed by the post quantization shape functions). It is worth noting that they differ from the imposed RTs (Figure 4c,d), due to the binary quantization procedure. To achieve a better matching between the imposed RT and the actual (post-quantization), it can be beneficial to set $\rho_3(\theta)$ constant, even beyond the considered work-range of angles, as shown in Figure 4b. Figure 5 illustrates the designed cluster.

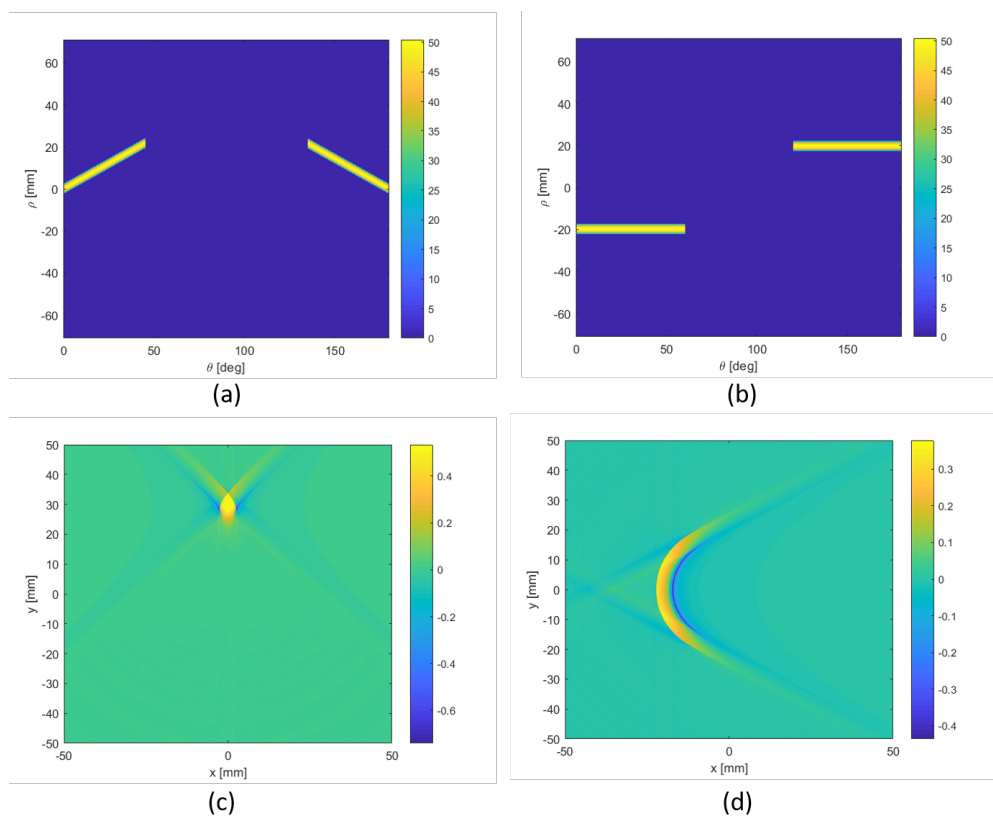


Figure 4. Cont.

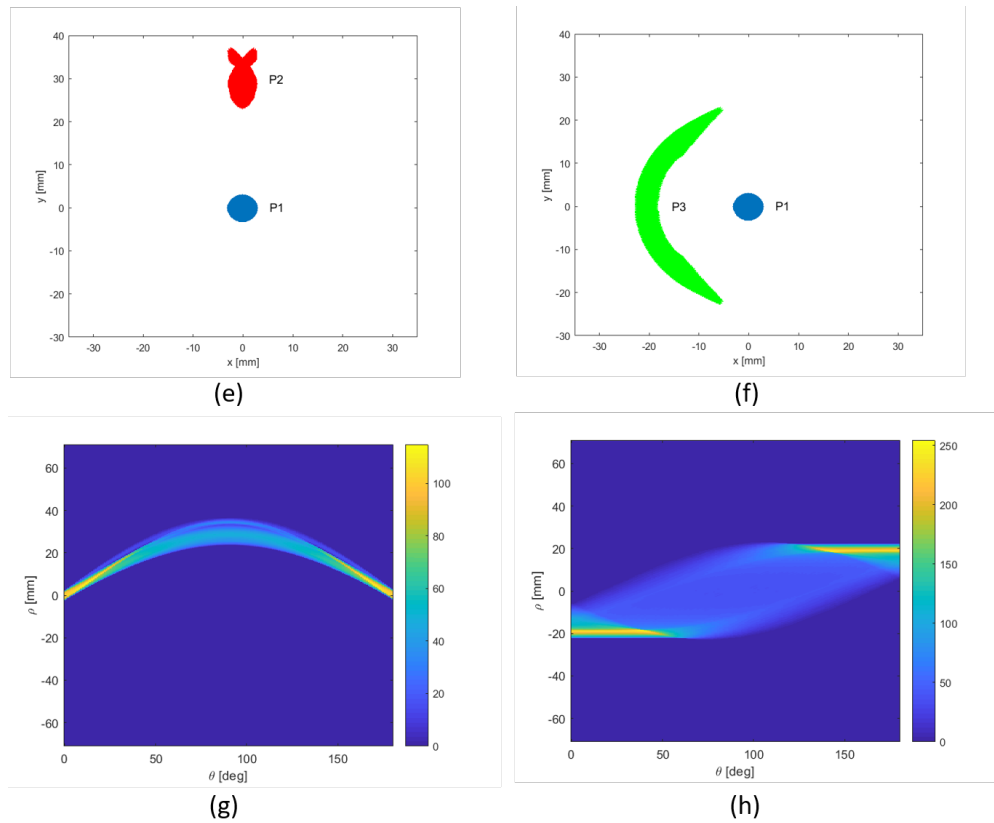


Figure 4. (a,b) Imposed RTs. (c,d) IRTs. (e,f) binary quantization of IRTs (Threshold values to binary quantization equal to 30% and 25% of maximum values of IRTs for sensors P2 and P3 respectively). (g,h) actual RTs. P2 and P3 are related to first and second column, respectively.

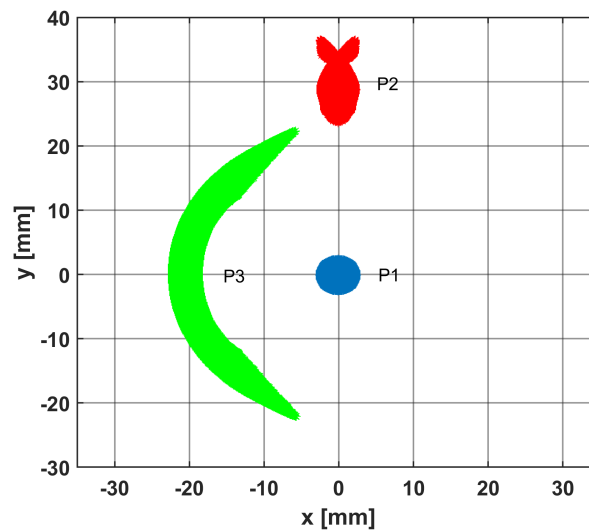


Figure 5. Designed cluster of three sensors: a reference circular sensor P1 and two reshaped sensors, P2 and P3.

4. Numerical Results and Discussion

In order to validate the design procedure and the proposed shaped sensors cluster, as represented in Figure 5, multiple impacts occurring on an aluminium plate (3 mm thick, Young’s modulus 70 GPa, Poisson’s coefficient 0.3 and material density 2700 Kg/m³) were simulated. The response of the shaped piezo-patches to impacts generating the fundamental antisymmetric mode (A_0) was computed using

the Greens function formalism adopted in [14]. An impulse response of a band pass Butterworth filter (10th order) with narrow bandwidth (i.e., 7.5 [KHz]) was used in order to emulate the actuated pulse. Subsequently, the estimated DToAs between P1 and P2, and the one between the P1 and P3 were computed by the locating the peak of the cross-correlation of acquired signals (i.e., the Maximum Likelihood (ML) estimator of DToA for measurements affected by additive white Gaussian noise (AWGN) with zero mean [11]), and their ratio $\Delta t_{12est} / \Delta t_{13est}$ was used to estimate the DoA (θ).

The ideal estimation function, linearly dependent with respect to the ratio $\Delta t_{12est} / \Delta t_{13est}$, could be obtained by inverting (5) with respect to θ . However, due to binary quantization procedure, the actual values of parameters α , ρ_0 and $\rho_3 c$ might be slightly different with respect to the imposed ones (6). In Figure 6, it can be seen that, when a narrow-band Lamb wave mode (e.g., A_0) is simulated, the relationship between the DToA ratio and the DoA (θ) is still linear. The parameters of the best-fit line, i.e., y-intercept m and slope q , can be computed by applying conventional linear regression procedures.

The estimated DoA (θ_{est}) as a function of its actual value (i.e., θ) for different working conditions is shown in Figures 7 and 8, when the A_0 mode propagation is simulated with $r = 0.4$ [m] as impacts distance. In particular, the two figures report the results at different values of sampling frequency (F_s) and at different values of Peak Signal to Noise Ratio (PSNR) when the measurements are affected by additive white Gaussian noise (AWGN) with zero mean, respectively. As can be seen, the DoA estimation is very accurate, with a standard deviation (SD) of DoA below three degrees, even when the measurements are affected by Gaussian noise (up to the PSNR = 18 dB) and the simulated "physical" sampling frequency is low (down to $F_s = 100$ KHz).

It is worth noting that:

1. In order to generate the Figure 7, the acquired signals were resampled (upsampling factor equal to 10) to improve the estimation accuracy of DToAs and so of DoA. The sampling rate conversion is the optimal method to reduce the uncertainty on DToAs (i.e., using *sinc* functions to interpolate), but the computational cost can be significant. In embedded systems, such onerous processing may be unfeasible. Possible alternatives consist in: (i) transmitting the acquired signals to a central processing unit (CPU) or (ii) using different interpolation techniques with reduced computational complexity, such as those proposed in [24,25].
2. The upper- and lower- bound errors that are displayed in Figure 7 are calculated by applying the propagation of uncertainty theory [26].
3. In the Figure 8, to numerically assess the SD of DoA, 1000 simulations were performed with measurements being affected by AWGN with zero mean, for each value of PSNR.

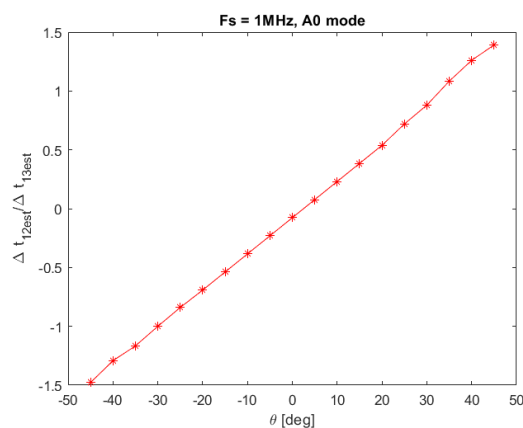


Figure 6. Estimated ratio of differences in time of arrival (DToAs) ($\Delta t_{12est} / \Delta t_{13est}$) with respect to the actual DoA (θ) for the case of A_0 mode propagating.

A numerical comparison of the performance in terms of SD between the conventional cluster of three circular sensors and the designed cluster is given in Table 1, assuming that measurements

are affected by AWGN with zero mean. The simulation of the A0 mode propagation was run when considering $r = 0.4$ [m] as impacts distance and $F_s = 1$ [MHz]. In order to assess the SD of DoA numerically, 1000 simulations were performed. The comparison is provided with the same maximum absolute value for the DToAs (i.e., d/v), so with the same memory requirement and same computational cost to estimate the time delays. As can be seen from Table 1, the SD value that is obtained with the cluster of shaped sensors is considerably reduced for all PSNR values.

Table 1. Comparison of Standard Deviation (SD) for the conventional cluster and proposed cluster of shaped sensors for noise-affected measurements at different Peak Signal to Noise Ratio (PSNR) values (SD Values are in [Deg]).

PSNR	Circular Sensors	Shaped Sensors
26 dB	1.61	0.95
22 dB	1.98	1.34
20 dB	2.35	1.76
19 dB	2.63	2.01
18 dB	3.08	2.78
17 dB	3.98	3.79

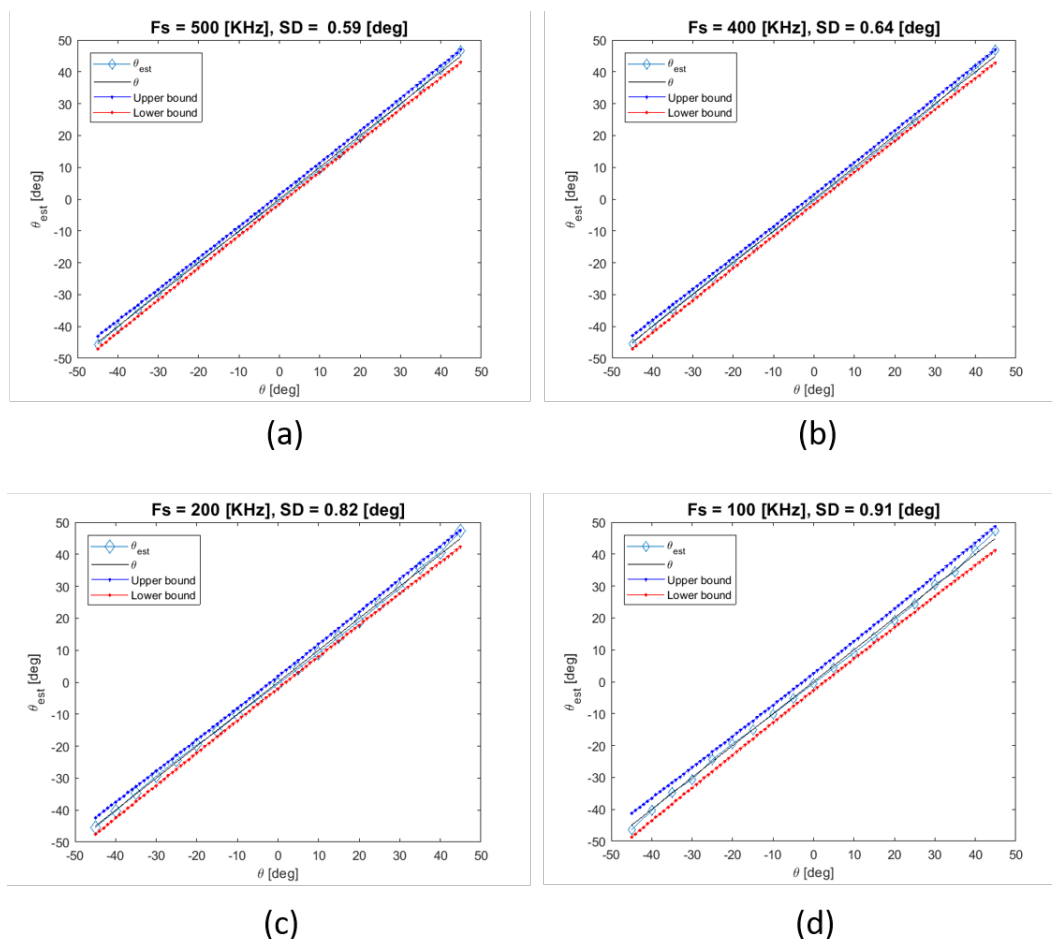


Figure 7. Estimated DoA (θ_{est}) with respect to the actual DoA (θ) at different sampling frequency values (indicated in the title of subplots, with the computed value of standard deviation of DoA) for the case of A0 mode propagating (the upper and lower bound limits computed according to the Propagation of Uncertainty theory on the basis of the ideal sensors geometries).

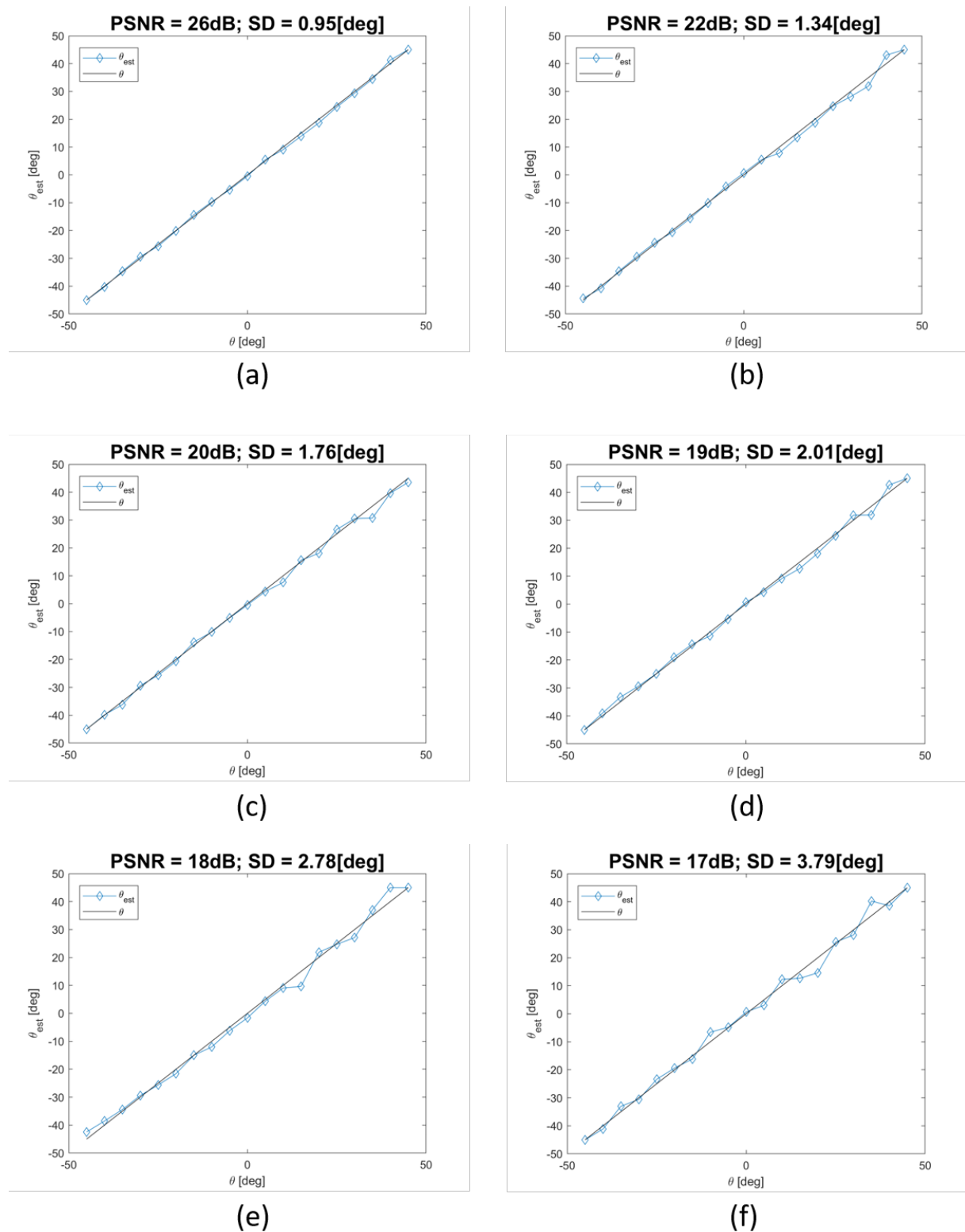


Figure 8. Estimated DoA (θ_{est}) with respect to the actual DoA (θ) for noise-affected measurements (additive white Gaussian noise) at different PSNR values (indicated in the title of subplots, with the computed value of standard deviation of DoA). The plotted results were computed by simulating the A_0 mode propagation, with $F_s = 1$ MHz.

5. Conclusions

In this work, a new shaped piezo-sensors cluster for direction of arrival (DoA) estimation of Lamb waves is proposed. The DoA estimation is performed by measuring the differences in time of arrival (DToAs) of the wave fronts between the sensors that belong to the cluster that is composed by three piezo patches. The shaping of the piezo-patches is designed, so that, given a reference sensor P1 (a piezo-disk), there is a linear dependence between the difference in time of arrival (DToA) of the wavefront between P1 and P2 and the DoA, whereas the DToA between P1 and P3 is constant across the considered range of DoA. In this way, the DoA estimation can be performed with reduced uncertainty and without knowing the actual wave mode velocity. The shaping of P2 and P3, which produces the mentioned relations between DToA and DoA, is achieved by exploiting the properties of the direct and inverse Radon Transform, in order to impose equal frequency amplitude responses for the sensors in the cluster. Therefore, the cross-correlation procedure can be used in order to estimate the DToAs between sensors. The numerical validation shows that the DoA estimation performance of the new designed cluster is very robust even when the sampling frequency and the signal to noise ratio decrease, and compares favorably with respect to conventional clusters of three circular sensors. Future developments include the validation of the numerical results with laboratory experiments.

Author Contributions: Conceptualization, M.D. and L.D.M.; methodology, M.D. and L.D.M.; software, M.D. and L.D.M.; validation, M.D.; formal analysis, M.D.; investigation, M.D.; resources, L.D.M.; data curation, M.D.; writing—original draft preparation, M.D.; writing—review and editing, L.D.M.; visualization, M.D.; supervision, L.D.M.; project administration, L.D.M.; funding acquisition, L.D.M. All authors have read and agreed to the published version of the manuscript.

Funding: This research was funded by the University of Bologna under the Proof of Concept project framework.

Conflicts of Interest: The authors declare no conflict of interest.

Abbreviations

The following abbreviations are used in this manuscript:

DoA	Direction of Arrival
DToA	Difference in Time of Arrival
FT	Fourier Transform
RT	Radon Transform
IRT	Inverse Radon Transform
MDDP	Maximum Difference in Distance of Propagation
SD	Standard Deviation
PSNR	Peak Signal to Noise Ratio
ML	Maximum Likelihood
F _s	Sampling Frequency
AWGN	Additive White Gaussian Noise
ADC	Analog to Digital Converter
CPU	Central Processing Unit

References

- Giurgiutiu, V.; Cuc, A. Embedded non-destructive evaluation for structural health monitoring, damage detection, and failure prevention. *Shock Vib. Dig.* **2005**, *37*, 83. [[CrossRef](#)]
- Putkis, O.; Dalton, R.; Croxford, A. The anisotropic propagation of ultrasonic guided waves in composite materials and implications for practical applications. *Ultrasonics* **2016**, *65*, 390–399. [[CrossRef](#)] [[PubMed](#)]
- Su, Z.; Ye, L.; Lu, Y. Guided Lamb waves for identification of damage in composite structures: A review. *J. Sound Vib.* **2006**, *295*, 753–780. [[CrossRef](#)]

4. Ciampa, F.; Meo, M. Acoustic emission source localization and velocity determination of the fundamental mode A0 using wavelet analysis and a Newton-based optimization technique. *Smart Mater. Struct.* **2010**, *19*, 045027. [[CrossRef](#)]
5. Staszewski, W.J.; Worden, K.; Wardle, R.; Tomlinson, G.R. Fail-safe sensor distributions for impact detection in composite materials. *Smart Mater. Struct.* **2000**, *9*, 298. [[CrossRef](#)]
6. Ciampa, F.; Meo, M. Impact detection in anisotropic materials using a time reversal approach. *Struct. Health Monit.* **2012**, *11*, 43–49. [[CrossRef](#)]
7. Chan, Y.T.; Ho, K. A simple and efficient estimator for hyperbolic location. *IEEE Trans. Signal Process.* **1994**, *42*, 1905–1915. [[CrossRef](#)]
8. Engholm, M.; Stepinski, T. Direction of arrival estimation of Lamb waves using circular arrays. *Struct. Health Monit.* **2011**, *10*, 467–480. [[CrossRef](#)]
9. Kundu, T. A new technique for acoustic source localization in an anisotropic plate without knowing its material properties. In Proceedings of the 6th European Workshop on Structural Health Monitoring, Dresden, Germany, 3–6 July 2012; pp. 3–6.
10. Kundu, T.; Nakatani, H.; Takeda, N. Acoustic source localization in anisotropic plates. *Ultrasonics* **2012**, *52*, 740–746. [[CrossRef](#)] [[PubMed](#)]
11. Van Der Heijden, F.; Duin, R.P.; De Ridder, D.; Tax, D.M. *Classification, Parameter Estimation and State Estimation: An Engineering Approach Using MATLAB*; John Wiley & Sons: Hoboken, NJ, USA, 2005.
12. Park, W.H.; Packo, P.; Kundu, T. Acoustic source localization in an anisotropic plate without knowing its material properties—A new approach. *Ultrasonics* **2017**, *79*, 9–17. [[CrossRef](#)] [[PubMed](#)]
13. Sen, N.; Kundu, T. A new wave front shape-based approach for acoustic source localization in an anisotropic plate without knowing its material properties. *Ultrasonics* **2018**, *87*, 20–32. [[CrossRef](#)] [[PubMed](#)]
14. De Marchi, L.; Testoni, N.; Marzani, A. Spiral-shaped piezoelectric sensors for Lamb waves direction of arrival (DoA) estimation. *Smart Mater. Struct.* **2018**, *27*, 045016. [[CrossRef](#)]
15. De Marchi, L.; Dibiase, M.; Testoni, N. Piezoelectric Sensors for Lamb Waves' Direction of Arrival (DoA) Estimation. *Proceedings* **2018**, *2*, 806. [[CrossRef](#)]
16. Bellan, F.; Bulletti, A.; Capineri, L.; Masotti, L.; Yaralioglu, G.G.; Degertekin, F.L.; Khuri-Yakub, B.; Guasti, F.; Rosi, E. A new design and manufacturing process for embedded Lamb waves interdigital transducers based on piezopolymer film. *Sens. Actuators A Phys.* **2005**, *123*, 379–387. [[CrossRef](#)]
17. Baravelli, E.; Senesi, M.; Gottfried, D.; De Marchi, L.; Ruzzene, M. Inkjet fabrication of spiral frequency-steerable acoustic transducers (FSATs). In *Health Monitoring of Structural and Biological Systems 2012*; International Society for Optics and Photonics: Bellingham, WA, USA, 2012; Volume 8348, p. 834817.
18. Baravelli, E.; Senesi, M.; Ruzzene, M.; De Marchi, L. Fabrication and characterization of a wavenumber-spiral frequency-steerable acoustic transducer for source localization in plate structures. *IEEE Trans. Instrum. Meas.* **2013**, *62*, 2197–2204. [[CrossRef](#)]
19. Giurgiutiu, V. Tuned Lamb wave excitation and detection with piezoelectric wafer active sensors for structural health monitoring. *J. Intell. Mater. Syst. Struct.* **2005**, *16*, 291–305. [[CrossRef](#)]
20. Ku, H.H. Notes on the use of propagation of error formulas. *J. Res. Natl. Bur. Stand.* **1966**, *70*, 263–273. [[CrossRef](#)]
21. Senesi, M.; Xu, B.; Ruzzene, M. Experimental characterization of periodic frequency-steerable arrays for structural health monitoring. *Smart Mater. Struct.* **2010**, *19*, 055026. [[CrossRef](#)]
22. Deans, S.R. *The Radon Transform and Some of Its Applications*; Courier Corporation: North Chelmsford, MA, USA, 2007.
23. Gaskill, J.D. *Linear Systems, Fourier Transforms, and Optics*; Wiley: New York, NY, USA, 1978; Volume 576.
24. Svilainis, L.; Lukoseviciute, K.; Dumbrava, V.; Chaziachmetovas, A. Subsample interpolation bias error in time of flight estimation by direct correlation in digital domain. *Measurement* **2013**, *46*, 3950–3958. [[CrossRef](#)]

25. Viola, F.; Walker, W.F. A spline-based algorithm for continuous time-delay estimation using sampled data. *IEEE Trans. Ultrason. Ferroelectr. Freq. Control* **2005**, *52*, 80–93. [[CrossRef](#)] [[PubMed](#)]
26. Le Maître, O.P.; Knio, O.M. Introduction: Uncertainty quantification and propagation. In *Spectral Methods for Uncertainty Quantification*; Springer: Berlin, Germany, 2010; pp. 1–13.

Publisher’s Note: MDPI stays neutral with regard to jurisdictional claims in published maps and institutional affiliations.



© 2020 by the authors. Licensee MDPI, Basel, Switzerland. This article is an open access article distributed under the terms and conditions of the Creative Commons Attribution (CC BY) license (<http://creativecommons.org/licenses/by/4.0/>).